Chemistry and Materials Research
ISSN 2224- 3224 (Print) ISSN 2225- 0956 (Online)
Vol.3 No.1, 2013

Role of Electrode Binder on Contact Formation between $La_{0.6}Sr_{0.4}CoO_{3-\alpha}$ Cathode and Yttrium Doped Cerate-Zirconate Solid Electrolyte

Nafisah Osman[1*] Mohd Azlan Mohd Ishak[1] Abdullah Abdul Samat[2]

1. Faculty of Applied Sciences, Universiti Teknologi MARA (UiTM), 02600 Arau, Perlis, Malaysia
2. Faculty of Applied Sciences, Universiti Teknologi MARA (UiTM), 40450 Shah Alam, Selangor, Malaysia

* E-mail of the corresponding author: fisha@perlis.uitm.edu.my

The research is financed by the Research Acculturation Collaborative Effort (RACE) Grant from the Ministry of Higher Education, Malaysia and the Excellent Fund Grant (DKCM) from Universiti Teknologi MARA.

Abstract

Powder of $La_{0.6}Sr_{0.4}CoO_{3-\alpha}$ (LSCO) was synthesized by a combined citrate-EDTA synthesis route. The high purity of LSCO cathode powder as confirmed by X-ray diffraction (XRD) analysis was prepared to become cathode slurries using different electrode binders namely polyvinyl alcohol (PVA), polyvinyl butyral-co-vinyl alcohol-co-vinyl acetate (PVB), polyvinyl pyrrolidone (PVP), ethyl cellulose (EC) and ethylene glycol (EG). These slurries were separately painted on the pellet surfaces of $BaCe_{0.54}Zr_{0.36}Y_{0.1}O_{2.95}$ (BCZY) solid electrolyte to fabricate symmetrical cell of LSCO/BCZY/LSCO. The role of electrode binder on contact formation between LSCO and BCZY was investigated. The contact formation at LSCO/BCZY interface was examined by Scanning Electron Microscope equipped with Electron Dispersive Spectroscopy (SEM/EDS). Three distinct areas corresponding to the LSCO cathode, BCZY electrolyte and LSCO/BCZY interface with free or crack/hole was observed in the SEM micrographs. The elemental compositions at these three areas were confirmed by EDS and their percentage was presented. The cells prepared with the aid of EC, EG, PVA and PVB showed poor contact between LSCO and BCZY due to the presence of the crack and/or hole (air gap) at interface except for the cell prepared with PVP. Therefore, PVP plays an important role in making a good contact between LSCO cathode and BCZY electrolyte.

Keywords: $La_{0.6}Sr_{0.4}CoO_{3-\alpha}$ cathode, $BaCe_{0.54}Zr_{0.36}Y_{0.1}O_{2.95}$ electrolyte, electrode binder, SEM/EDS

1. Introduction

The past decade has witnessed the extensive efforts towards development of intermediate temperature solid oxide fuel cell (IT-SOFC). It is deemed to play an important role in future clean power generation as it offers low pollutant emission, high energy conversion efficiency and excellent fuel flexibility. However, IT-SOFC has very important limitation due to the voltage drop in the internal components caused by increasing of polarization resistance at cathode/electrolyte interface at intermediate temperatures (500-800 °C) (Perez-Coll *et al*. 2008; Chen *et al*. 2009). Since the performance of IT-SOFC is strongly relies on the properties of the cathode/electrolyte interface then to overcome this limitation, two approaches can be adopted namely by using mixed ionic-electronic conductor (MIEC) cathode materials and optimizing cathodic structure of the cell (Qiang *et al*. 2009).

For the first approach, currently MIEC perovskite-type oxides $Ln_{1-x}A_xMO_{3-\alpha}$ (Ln: La, Sm, Nd; A: Ca, Sr, Ba; M: Co, Fe, Ni) materials are widely being used as cathode materials for IT-SOFC (Jin *et al*. 2008; Chen *et al*. 2009; Ghouse *et al*. 2010). Among these perovskite-type oxides materials, $La_{0.6}Sr_{0.4}CoO_{3-\alpha}$ (LSCO) has been considered as one of the most promising cathode candidates for IT-SOFC as it has shown good performance with low polarization resistance, higher electronic conductivity and good catalytic activity at intermediate temperatures (Tao *et al*. 2008; Berenov *et al*. 2010). An economical way to synthesize this perovskite-type oxide powder is via a combined citrate-EDTA method. The advantages of this method are high purity of powders can be obtained at relatively low temperatures and excellent stoichiometry control during synthesizing process. There are two basic chemical reactions involve in this method namely (i) complexation or chelation between metal ions and chelating agents (citric acid and EDTA) and (ii) poly-esterification of complexes with polymerizing agent (ethylene glycol).

For the second approach, optimizing cathodic structure can be done via fabrication process. The fabrication process

of IT-SOFC cell should be optimized as formation of reaction products, inter-diffusion, segregation and electronic changes at the interface will definitely affect IT-SOFC performance (Kostogloudis *et al*. 2000; Backhaus-Ricoult 2008). Fabrication parameters such as selection of electrode binders (additives) must be investigated. Electrode binders which usually a polymer helps to keep the cathode materials bind onto the electrolyte surfaces (Choudhury *et al*. 2011; Munao *et al*. 2011). A good contact or strong adhesion between cathode and electrolyte at cathode/electrolyte interface is definitely needed to ensure the integrity of the cell performance and may reduce the deleterious effect upon the transport of ions in polycrystalline materials and crucial for the good performance of cell (Choi *et al*. 2002; Jacobson 2010). Although tremendous studies have been devoted to the interaction or inter-diffusion between zirconia and La-based cathode materials, but less detailed investigation has been performed on the selection and role of the electrode binder in making a good contact between LSCO cathode and $BaCe_{0.54}Zr_{0.36}Y_{0.1}O_{2.95}$ (BCZY) electrolyte. Therefore, it is essential to study the role of electrode binder on contact formation between LSCO and BCZY. The outcomes from this study may contribute to the significant knowledge in optimizing fabrication process in order to produce high performance IT-SOFC.

2. Experimental Procedure

2.1 Synthesis and Characterization of LSCO Powder

The LSCO cathode powder was prepared using a combined citrate-EDTA synthesis route. Citric acid (CA) and ethylenediaminetetraacetic acid (EDTA) was employed as chelating agents. To yield 5 g of final LSCO powder, a stoichiometric amount of $La(NO_3)_3.6H_2O$ (99.999% purity, ACROS), $Sr(NO_3)_2$ (99+% purity, ACROS), $Co(NO_3)_2.6H_2O$ (99+% purity, ACROS) and citric acid monohydrate, (CA) (99.5% purity, MERCK) in 1:1.5 molar ratio (Metal nitrates, M^+ : CA) were first dissolved in 100 mL deionized water. The transparent red color solution was heated in a water bath at 75 °C for an hour under magnetic agitation. The calculated amount of EDTA (99% purity, ACROS) with molar ratio to overall metal cations content of 0.5:1 was added into the solution. The color of the solution was turned to dark violet after a few minutes. After that, the pH of the solution was adjusted to be 0.5 by adding appropriate amount of ammonia hydroxide solution (25% assays, HmbG®). Then, ethylene glycol (EG) (99.97% purity, ACROS) with molar ratio to overall metal cations contents of 3:1 was added. In this synthesis route, EG was used as surfactant for polymerization process of metal complexes. The solution was continuously stirred and heated for several hours. Next, the resulting viscous gel was dried at 150 °C for 12 hours and at 250 °C for 5 hours. The dried gel was calcined at selected temperatures which are 800 °C, 900 °C and 1000 °C with heating/cooling rate of 10 °C min^{-1} for 5 hours to yield black powder. The obtained black powder was grounded and its phase identification was examined by X-ray diffractometer (XRD 6000 Shimadzu). The XRD was operating at 40 kV and 30 mA using a step procedure of 0.02 s^{-1} for the 2θ range from 20° to 80°.

2.2 Preparation of LSCO Cathode Slurry

The electrode binders used in preparation of LSCO cathode slurries were polyvinyl alcohol, PVA (average M_w 9000-10000, 80% hydrolyzed, ALDRICH), polyvinyl butyral-co-vinyl alcohol-co-vinyl acetate, PVB (average M_w 50000-80000 by GPC, ALDRICH), polyvinyl pyrrolidone, PVP (M_w 160000, R&M), ethyl cellulose, EC (M_w 40000, ALDRICH) and ethylene glycol, EG (M_w 62.06, ACROS). A molecular structure of each binder is shown in Figure 1. The calcined LSCO powders were ground and mixed with different electrode binders in ethanol with ratio of 10:1:20. The mixtures were stirred for 30 minutes and dispersed homogeneously by an ultrasonic bath for 30 minutes.

2.3 Fabrication and Characterization of symmetrical cell

The calcined BCZY powder was sintered at 1400 °C for 10 hours to produce BCZY pellet as reported previously by Osman et *al*. (2009). Both sides of the pellet were polished with 1000# SiC grit paper and ultrasonically cleaned. The respective prepared LSCO cathode slurry was brushed onto both sides of the sintered BCZY pellet. The symmetrical cell was first heated up to 500 °C to eliminate the electrode binder and then to 950 °C for 2 hours. Next, the symmetrical cell was cross-sectional mounted in different sample holders using epoxy resin. The mounted cells were polished using 1200#, 1500# and 2000# SiC grit papers. Contamination on the surface of the cells was ultrasonically cleaned after each step. Afterward, the cells were polished using 6 μm diamond polish to ensure a

scratch free surface area. The polishing process was finished by using 1 μm diamond polish and the cells were dried in air for few hours. The same procedure was also applied for the sintered BCZY electrolyte pellet painted with platinum (Pt) ink which serves as a standard cell. All the cells were coated with thin films of gold and examined by Carl Zeiss SMT Supra 40VP Scanning Electron Microscope (SEM) equipped with OXFORD INCA X-Act Electron Dispersive Spectroscopy (EDS) to observe the surface morphology and determine the elemental compositions at cathode, electrolyte and interface areas. The areas were denoted as area 1 (cathode), area 2 (electrolyte) and area 3 (interface). Imaging was performed in Secondary Electron (SEI) mode only using an accelerating voltage of 10 kV.

3. Results and Discussion

3.1 XRD analysis

Figure 2 shows the XRD patterns of LSCO powders calcined at 800 °C, 900 °C and 1000 °C for 5 hours with heating/cooling rate of 10 °C min^{-1}. The peaks intensity in all XRD patterns was increased as the calcination temperatures increased. The strongest peaks of the XRD patterns matched with JCPDS file 48-0121 were found in all spectra that indicate the formation of perovskite phase. The presence of additional peaks was also observed in XRD patterns of the powders calcined at 800 °C and 900 °C. These peaks correspond to trace of impurity phases including cobalt oxide (CoO) (JCPDS file 43-1004) and strontium cobalt oxide ($SrCoO_x$) (JCPDS file 49-0692).

However, these impurity phases were disappeared when the powder was calcined at 1000 °C indicating that it was fully developed into a single perovskite phase of LSCO. The result obtained is in agreement with the work done by Bansal & Zhong (2006) which synthesize the LSCO powder via combustion synthesis method.

3.2 SEM/EDS analysis

SEM micrograph of cross-sectional view at interface between platinum (Pt) and BCZY electrolyte is shown in Figure 3. Pt serves as reference electrode since it is a pure electronic conductor due to its high catalytic and stability in oxidative and reductive atmosphere. Based on the SEM micrograph, it is observed that Pt (area 1) was not well adhered onto the BCZY (area 2) as hole or air gap was being observed at Pt/BCZY interface (area 3). This is due to Pt and BCZY are in different class of materials which are metal and ceramic, accordingly. The joint between metal-ceramic is difficult to bring in a good contact without provided appropriate parameters such as temperature, time and pressure (Allen & Borbidge 1983; Tomsia 1993). The elemental composition at these three areas was analyzed by EDS. The results confirmed that the area 1 is Pt, area 2 is BCZY and area 3 is the hole or air gap as no any element was detected as shown in Table 1.

SEM micrographs in Figure 4 show the contact formation at LSCO/BCZY interface with the aid of various electrode binders namely EC, EG, PVA and PVB. Three distinct areas corresponding to the LSCO cathode, BCZY electrolyte and interface layer that consists of crack/hole or air gap can be clearly seen from the micrographs. The respective areas were denoted as area 1 (LSCO), area 2 (BCZY) and area 3 (interface) and elemental composition at each area was confirmed by EDS as shown in Table 2. Figure 4(a) depicts the contact at LSCO/BCZY interface which used EC as electrode binder. EC is a conventional electrode binder used in strontium-doped lanthanum manganite, $La_{1-x}Sr_xMnO_{3-\alpha}$ (LSM) cathode slurry to paste on yttria-stabilized zirconia (YSZ) electrolyte pellet by a screen printing (Qiang *et al*. 2009). However, in this work, by manually painted, the LSCO was not thoroughly adhered onto BCZY electrolyte since cracking along the interface was noticed (as clearly shown in the insert in Figure 4(a)). The reason for the cracking is could be due to some thermal expansion mismatch at the interface during firing process. Furthermore, difference in particle packing is also can lead to crack formation (Dong 1990). At the earlier stage of the binder removal, the surface of the LSCO and BCZY materials might be expanded by the interior part due to a more advanced stage of the binder removal. This expansion will proceed until there is no sufficient liquid binder to supply lubricity for the rearrangement process. As the interior binder is lost, the materials are pulled into denser packing by capillary forces. At the same time, the exterior particle layer tends to resist the process of densification resulting to the formation of crack.

For the cathode slurry prepared with EG and PVA, a relatively large hole at LSCO/BCZY interface is clearly being observed in the SEM micrograph as shown in Figure 4(b) and Figure 4(c). EG and PVA possess same functional group as ethanol (solvent) in their molecular structures which is hydroxyl group (-OH). For EG, the formation of the

hole at interface might be due to the EG was swollen as it dissolves in ethanol. When the amount of EG was larger than the equilibrium solvent content, it will start to swell. Then, after it was burnt out, the large hole will form as the consequence of the swollenness at the beginning of the process (Kurokawa *et al*. 2007). The same process might also happen to the PVA which is a cheap, non-toxic and chemically stable polymer. Additionally, PVA cannot be used in fuel cells that use aqueous solutions as fuel and/or oxidant because of its high solubility in water (Choudhury *et al*. 2011).

Figure 4(d) shows the contact at LSCO/BCZY interface which used PVB as electrode binder. PVB is a product of reaction between PVA and butyraldehyde in the presence of an acid as medium. The final structure can be considered to be a random copolymer of vinyl butyral, vinyl alcohol and vinyl acetate. It consists of two widely different types of units which are (i) vinyl alcohol (polar and hydrophilic) and (ii) vinyl butyral (hydrophobic) and has ether (C-O-C) functional group in its structure. From the micrograph, PVB does not aid in making a good contact between LSCO and BCZY since the hole or air gap was appeared at interface region. This might happened due the PVB is not well dissolved in ethanol as the presence of hydrophobic part in its structure limits the interaction between ethanol, LSCO, BCZY and PVB itself. Another reason is might due to the incomplete removal of carbonaceous species in PVB binder during its decomposition that leads to high content of carbon residue in the final product (Shende *et al*. 2001). As shown in the Table 2, PVB has the highest percentage of carbon residue as compared to other electrode binders.

SEM micrograph of cross-sectional view at LSCO/BCZY interface with the aid of PVP binder is shown in Figure 5. No obvious crack and hole or air gap appeared at the interface. It shows a good adhesion between LSCO and BCZY. The PVP has amide group in its structure. The available lone electron pairs of oxygen and nitrogen atoms in its structure can interact with the metal ions in LSCO and BCZY materials. During the early stage of evaporation process of solvent which is the ethanol, metal ions in both materials adsorb on PVP surface. After that, the binder was burnt out and the aggregation at LSCO/BCZY interface was took place to form a good contact (Shao *et al*. 2000). Data of elemental atomic percentage observed for area 1 to area 3 are tabulated in Table 3. It can be seen that the interfacial layer is composed of lanthanum (La), barium (Ba) and cerium (Ce).

All the results obtained from EDS showed that a relatively high percentage of carbon was detected. The reason is the electrode binders retain high number of carbons and they will produce a large amount of carbon residue if the combustion process is not carried out in sufficient oxygen. During the firing process, most of the organic binder which is added to the ceramic powders to improve their workability decomposes within the temperature range of 200 °C to 500 °C. This is the reason why we have to first heat up the cell at 500 °C. Then, small amount of carbonaceous residue formed by binder decomposition remains in the fired cell. This carbon residue need to be removed before sintering of the cell commences, otherwise the carbon residue remaining in the cell may alter the desired properties including porosity of the final product (Tomsia 1993; Shende *et al*. 2001). Carbon content could be further minimized by increasing the firing temperature and time.

The elemental composition percentage of some elements such as yttrium (Y) was not presented even though the peaks of Y appeared in all EDS spectra as shown in Figure 6. The reason is due to the position of major line of Y should appear has been overlapped with other elements such as strontium (Sr) and zirconium (Zr). It is corresponding to X-rays generated by these three element are in the same energy-level shells (K, L and M).

The discrepancy in microstructure at cathode/electrolyte interface that prepared with different electrode binders might due to the presence of the different functional groups in their molecular structure. Besides that, the hydrophobic and hydrophilic properties possess by each binder are also contribute to the results obtained. In the other words, the contents of binder in cathode matrixes are important to keep the cathode intact and bound onto the electrolyte surface (Choudhury *et al*. 2011). Additionally, others parameters such as the amounts of binder, heat treatment temperatures and choice of solvent used need to be considered when dealing with fabrication of the cell which consisting of different cathode and electrolyte materials. Mechanical measurements in combinations with in-situ microscopic observations and binding mechanism are needed to further understand the role of the electrode binder in optimizing the polarization of electrode-electrolyte in order to increase the efficiency of cell performance.

4. Conclusion

This study has revealed that electrode binder play an important role in helping to make a good contact at LSCO/BCZY interface. Among all the electrode binders used in this study, the LSCO cathode prepared with PVP binder showed a good adherence onto BCZY electrolyte surface. Therefore, PVP is considered to be the preferable electrode binder to obtain uniform microstructures and high performance for the LSCO cathode. Further and detail works on the chemical compatibility and performance of LSCO cathode co-sintering with BCZY electrolyte to be used for IT-SOFC components have been extensively investigated and the progress will be reported elsewhere.

References

Allen, R., & Borbidge, W. (1983). Solid state metal-ceramic bonding of platinum to alumina. *Journal of Materials Science 18* , 2835-2843.

Backhaus-Ricoult, M. (2008). SOFC - A playground for solid state chemistry. *Solid State Sciences 10* , 670-688.

Bansal, N. P., & Zhong, Z. (2006). Combustion synthesis of $Sm_{0.5}Sr_{0.5}CoO_{3-x}$ and $La_{0.6}Sr_{0.4}CoO_{3-x}$ nanopowders for solid oxide fuel cell cathodes. *Journal of Power Sources 158* , 148-153.

Berenov, A., Atkinson, A., Kilner, J., Bucher, E., & Sitte, W. (2010). Oxygen tracer diffusion and surface exchange kinetics in $La_{0.6}Sr_{0.4}CoO_{3-\delta}$. *Solid State Ionics 181* , 819-826.

Chen, J., Liang, F., Liu, L., Jiang, S. P., & Jian, L. (2009). Characterization and evaluation of $La_{0.8}Sr_{0.2}Co_{0.8}Ni_{0.2}O_{3-\delta}$ prepared by a polymer-assisted combustion synthesis as a cathode material for intermediate temperature solid oxide fuel cells. *International Journal of Hydrogen Energy 34* , 6845-6851.

Choi, N.-S., Lee, Y.-G., & Park, J.-K. (2002). Effect of cathode binder on electrochemical properties of lithium rechargeable polymer batteries. *Journal of Power Sources 112* , 61-66.

Choudhury, N. A., Ma, J., Sahai, Y., & Buchheit, R. G. (2011). High performance polymer chemical hydrogel-based electrode binder materials for direct borohydride fuel cells. *Journal of Power Sources 196* , 5817-5822.

Dong, C. (1990). *Binder removal in ceramics. PhD thesis.* Massachusets Institute of Technology.

Ghouse, M., Al-Yousef, Y., Al-Musa, A., & Al-Otaibi, M. (2010). Preparation of $La_{0.6}Sr_{0.4}Co_{0.2}Fe_{0.8}O_3$ nanoceramic cathode powders for solid oxide fuel cell (SOFC) application. *International Journal of Hydrogen Energy 35* , 9411-9419.

Jacobson, A. J. (2010). Materials for Solid Oxide Fuel Cells. *Chem. Mater. 22* , 660-674.

Jin, C., Liu, J., Guo, W., & Zhang, Y. (2008). Electrochemical characteristics of an $La_{0.6}Sr_{0.4}Co_{0.2}Fe_{0.8}O_3$-$La_{0.8}Sr_{0.2}MnO_3$ multi-layer composite cathode for intermediate-temperature solid oxide fuel cells. *Journal of Power Sources 183* , 506-511.

Kostogloudis, G. C., Ftikos, C., Ahmad-Khanlou, A., Naomidis, A., & Stover, D. (2000). Chemical compatibility of alternative perovskite oxide SOFC cathodes with doped lanthanum gallate solid electrolyte. *Solid State Ionics 134* , 127-138.

Kurokawa, H., Lau, G. Y., Jacobson, C. P., Jonghe, L. C., & Visco, S. J. (2007). Water-based binder system for SOFC porous steel substrates. *Journal of Materials Processing Technology 182* , 469-476.

Munao, D., Erven, J. v., Valvo, M., Garcia-Tamayo, E., & Keldet, E. (2011). Role of the binder on the failure mechanism of Si nano-composite electrodes for Li-ion batteries. *Journal of Power Sources 196* , 6695-6702.

Osman, N., Talib, I., & Hamid, H. (2009). Heat treatment and characterization of Yb doped barium cerate prepared via sol-gel technique. *Journal Sains Malaysiana 38(1)* , 103-107.

Perez-Coll, D., Aguadero, A., Escudero, M., Nunez, P., & Daza, L. (2008). Optimization of the interface polarization of the La_2NiO_4-based cathode working with the $Ce_{1-x}Sm_xO_{2-\delta}$ electrolyte system. *Journal of Power Sources 178* , 151-162.

Qiang, F., Sun, K., Zhang, N., Le, S., Zhu, X., & Piao, J. (2009). Optimization on fabrication and performance of A-site-deficient $La_{0.58}Sr_{0.4}Co_{0.2}Fe_{0.8}O_{3-\delta}$ cathode for SOFC. *J Solid State Electrochem 13* , 455-467.

Shao, Z., Xiong, G., Ren, Y., Cong, Y., & Yang, W. (2000). Low temperature synthesis of perovskite oxide using the adsorption properties of cellulose. *Journal of Materials Sciences 35* , 5639-5644.

Shende, R. V., Krueger, D. S., & Lombardo, S. J. (2001). Supercritical extraction of binder containing poly (vinyl butyral) and dioctyl phthalate from barium titanat-platinum multilayer ceramic capacitors. *Journal of Material Science: Materials in Electronics 12* , 637-643.

Tao, Y., Shao, J., Wang, J., & Wang, W. G. (2008). Synthesis and properties of $La_{0.6}Sr_{0.4}CoO_{3-\alpha}$ nanopowder. *Journal of Power Sources 185* , 609-614.

Tomsia, A. (1993). Ceramic/metal joining for structures and materials. *Journal de Physique IV: Colloque C7, suppllement au Journal de Physique III, Volume 3* , 1317-1326.

Table 1: EDS data of elemental atomic percentage observed for areas 1 to 3 at Pt/BCZY interface

Element	Elemental atomic percentage for indicated position on SEM micrograph (%)		
	Area 1	Area 2	Area 3
C	44.73	25.32	-
O	-	40.13	-
Pt	55.27	-	-
Ba	-	18.34	-
Ce	-	11.20	-
Zr	-	5.01	-
Y	-	-	-

Table 2: EDS data of elemental atomic percentage observed for areas 1 to 3 at LSCO/BCZY interface with the aid of various electrode binders

Element	Elemental atomic percentage for indicated position on SEM micrograph (%)											
	Area 1				Area 2				Area 3			
	EC	EG	PVA	PVB	EC	EG	PVA	PVB	EC	EG	PVA	PVB
C	54.32	57.42	43.80	60.69	45.75	40.64	34.12	47.92	-	-	-	-
O	35.11	38.79	39.19	23.40	44.28	43.05	45.37	36.87	-	-	-	-
La	2.26	0.31	4.55	5.35	-	-	-	-	-	-	-	-
Sr	2.69	0.54	3.79	3.76	-	-	-	-	-	-	-	-
Co	5.63	2.94	8.67	6.80	-	-	-	-	-	-	-	-
Ba	-	-	-	-	6.85	11.18	13.13	10.84	-	-	-	-
Ce	-	-	-	-	3.12	5.13	6.07	4.37	-	-	-	-
Zr	-	-	-	-	-	-	1.32	-	-	-	-	-
Y	-	-	-	-	-	-	-	-	-	-	-	-

Table 3: EDS data of elemental atomic percentage observed for areas 1 to 3 at LSCO/BCZY interface with the help of PVP electrode binder

Element	Elemental atomic percentage for indicated position on SEM micrograph (%)		
	Area 1	Area 2	Area 3
C	49.79	23.94	44.37
O	31.05	44.89	36.94
La	4.98	-	3.16
Sr	3.74	-	-
Co	10.44	-	-
Ba	-	17.92	9.52
Ce	-	9.08	6.02
Zr	-	4.17	-
Y	-	-	-

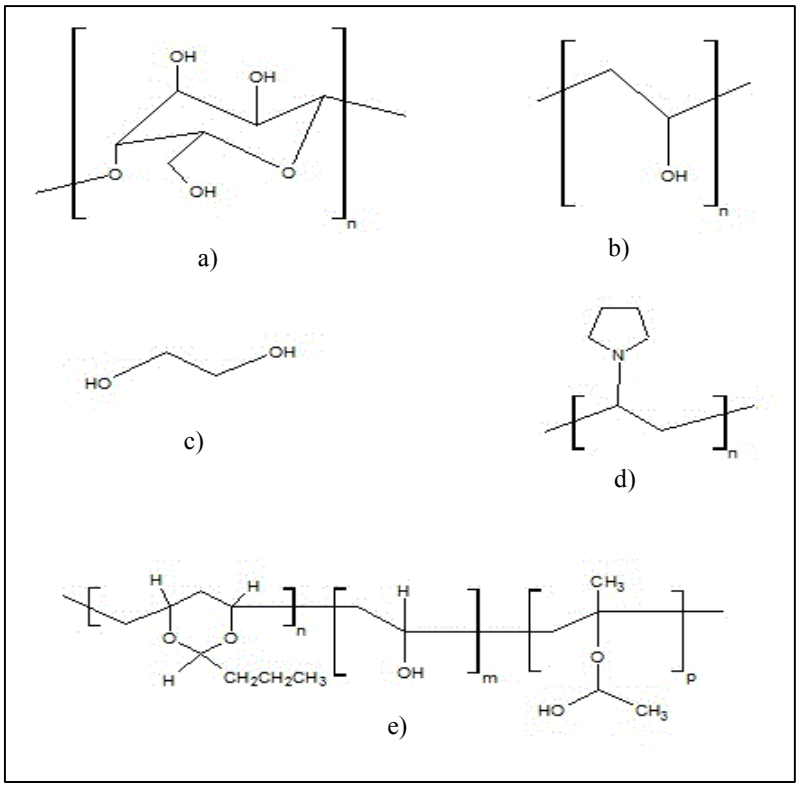

Figure 1. Molecular structure of: EC (a); PVA (b); EG (c); PVP (d) and PVB (e)

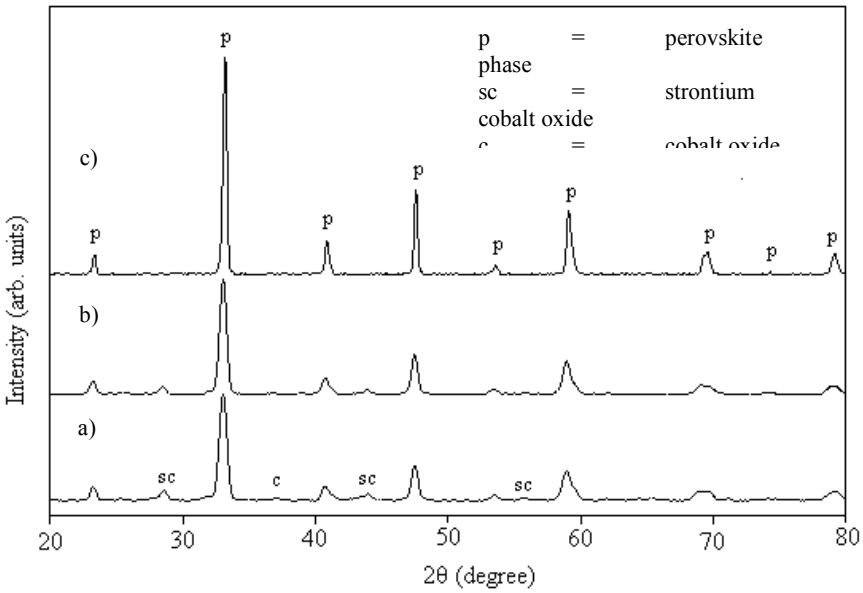

Figure 2. XRD patterns of LSCO powders calcined at: 800 °C (a); 900 °C (b) and 1000 °C (c)

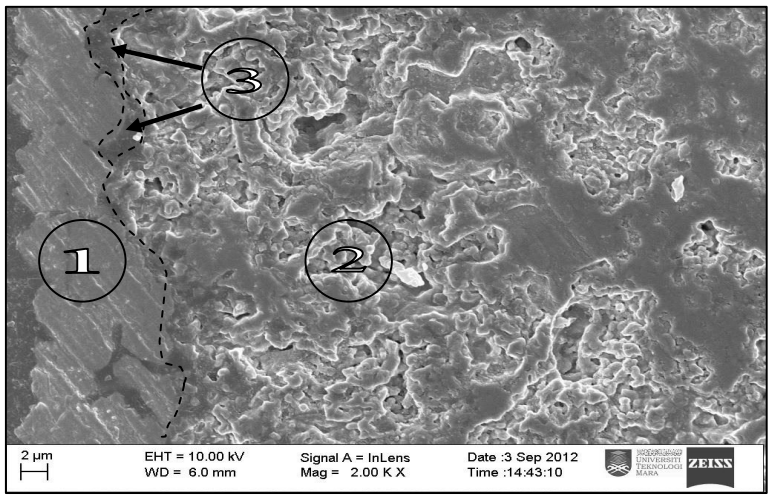

Figure 3. SEM micrograph of cross-sectional view at Pt/BCZY interface (area 1 = Pt; area 2 = BCZY; area 3 = interface with hole/air gap)

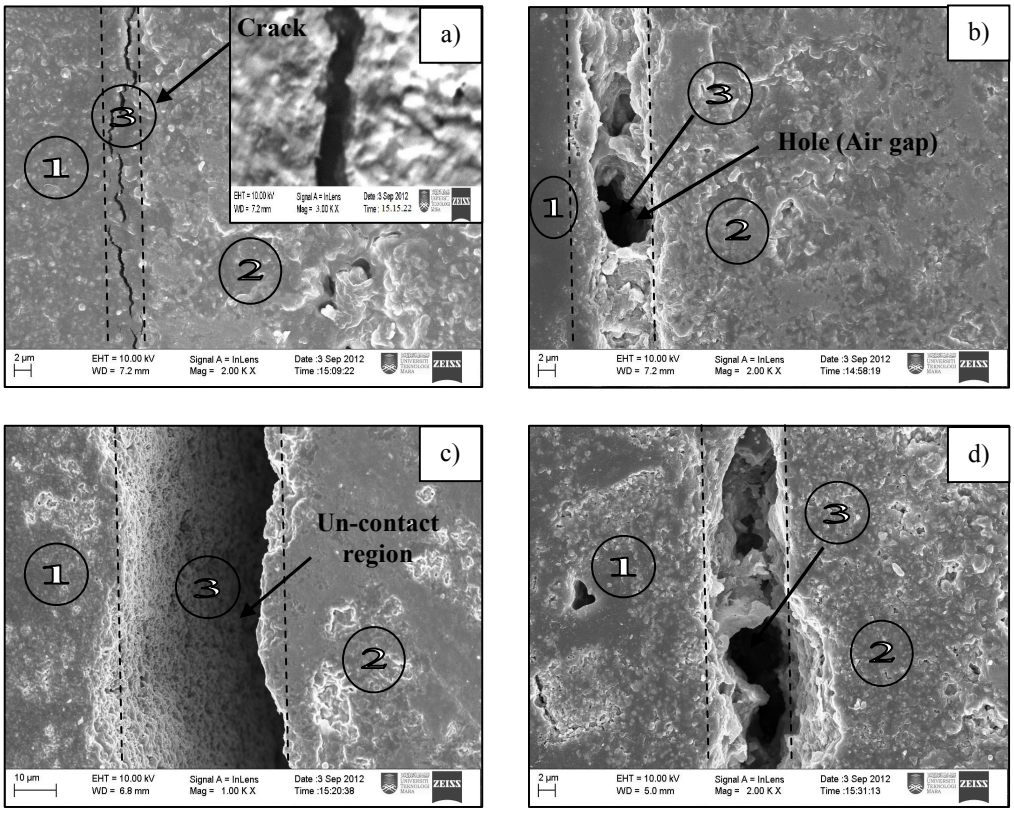

Figure 4. SEM micrographs of cross-sectional view of contact formation at LSCO/BCZY interface with the aid of various electrode binders: EC (a); EG (b); PVA (c) and PVB (d)
(area 1 = LSCO; area 2 = BCZY; area 3 = interface with crack/hole/air gap)

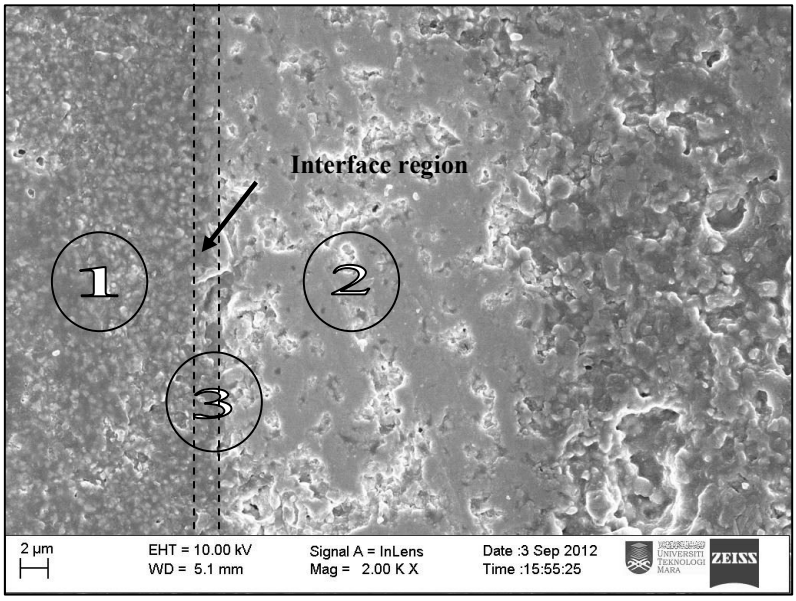

Figure 5. SEM micrograph of cross-sectional view of contact formation at LSCO/BCZY interface with the help of PVP electrode binder

(area 1 = LSCO; area 2 = BCZY; area 3 = LSCO/BCZY interface)

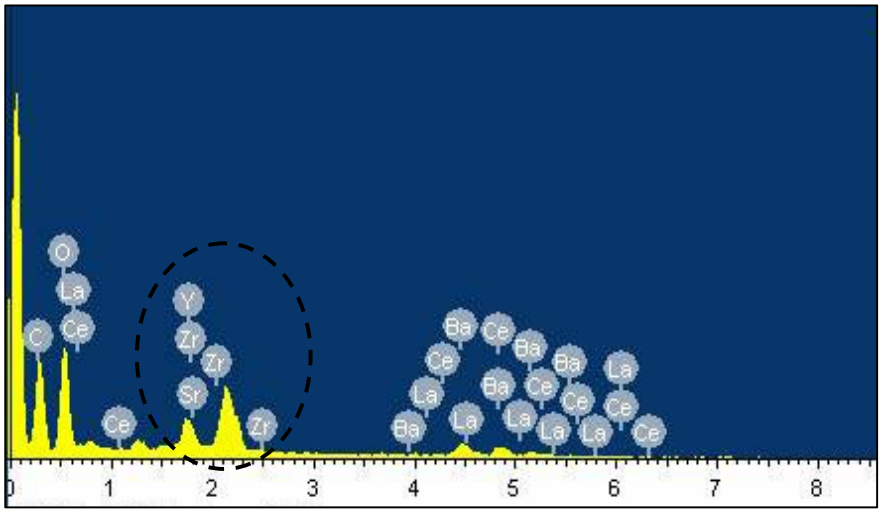

Figure 6. EDS spectrum of Zirconium (Zr) and Yttrium (Y) with other elements

This academic article was published by The International Institute for Science, Technology and Education (IISTE). The IISTE is a pioneer in the Open Access Publishing service based in the U.S. and Europe. The aim of the institute is Accelerating Global Knowledge Sharing.

More information about the publisher can be found in the IISTE's homepage: http://www.iiste.org

CALL FOR PAPERS

The IISTE is currently hosting more than 30 peer-reviewed academic journals and collaborating with academic institutions around the world. There's no deadline for submission. **Prospective authors of IISTE journals can find the submission instruction on the following page:** http://www.iiste.org/Journals/

The IISTE editorial team promises to the review and publish all the qualified submissions in a **fast** manner. All the journals articles are available online to the readers all over the world without financial, legal, or technical barriers other than those inseparable from gaining access to the internet itself. Printed version of the journals is also available upon request of readers and authors.

IISTE Knowledge Sharing Partners

EBSCO, Index Copernicus, Ulrich's Periodicals Directory, JournalTOCS, PKP Open Archives Harvester, Bielefeld Academic Search Engine, Elektronische Zeitschriftenbibliothek EZB, Open J-Gate, OCLC WorldCat, Universe Digtial Library , NewJour, Google Scholar